



Universiteit
Leiden
The Netherlands

Analytical chemistry and biochemistry of glycosphingolipids : new developments and insights

Mirzaian, M.

Citation

Mirzaian, M. (2017, June 14). *Analytical chemistry and biochemistry of glycosphingolipids : new developments and insights*. Retrieved from <https://hdl.handle.net/1887/49552>

Version: Not Applicable (or Unknown)

License: [Licence agreement concerning inclusion of doctoral thesis in the Institutional Repository of the University of Leiden](#)

Downloaded from: <https://hdl.handle.net/1887/49552>

Note: To cite this publication please use the final published version (if applicable).

Cover Page



Universiteit Leiden



The handle <http://hdl.handle.net/1887/49552> holds various files of this Leiden University dissertation

Author: Mirzaian, Mina

Title: Analytical chemistry and biochemistry of glycosphingolipids : new developments and insights

Issue Date: 2017-06-14

Chapter 12

Lyso-glycosphingolipid abnormalities
in different murine models of
lysosomal storage disorders

Mol Genet Metab. 2016 Feb;117(2):186-93

Lyso-glycosphingolipid abnormalities in different murine models of lysosomal storage disorders

Maria J. Ferraz ^{a,1}, André R.A. Marques ^{a,1}, Paulo Gaspar ^{b,c,d,1}, Mina Mirzaian ^{e,1}, Cindy van Roomen ^a, Roelof Ottenhoff ^a, Pilar Alfonso ^f, Pilar Irún ^f, Pilar Giraldo ^f, Patrick Wisse ^g, Clara Sá Miranda ^{b,c}, Herman S. Overkleeft ^g, Johannes M. Aerts ^{a,e,*}

^a Department of Medical Biochemistry, Academic Medical Center, 1105, AZ, Amsterdam, The Netherlands

^b Organelle Biogenesis & Function Group, Instituto de Investigação e Inovação em Saúde (I3S), 4200-135 Porto, Portugal

^c Lysosome and Peroxisome Biology Unit (UniLiPe), Institute of Molecular and Cell Biology (IBMC), Universidade do Porto, 4150-180 Porto, Portugal

^d Instituto de Ciências Biomédicas Abel Salazar (ICBAS), Universidade do Porto, 4050-313 Porto, Portugal

^e Department of Medical Biochemistry, Leiden Institute of Chemistry, Leiden University, 2333, CC, Leiden, The Netherlands

^f Centro de Investigación Biomédica en Red de Enfermedades Raras, Unidad de Investigación Translacional, Zaragoza, Spain

^g Department of Bio-organic Synthesis, Leiden Institute of Chemistry, Leiden University, 2333, CC, Leiden, The Netherlands

ARTICLE INFO

Article history:

Received 15 November 2015

Received in revised form 21 December 2015

Accepted 21 December 2015

Available online 23 December 2015

Keywords:

Gaucher disease

Fabry disease

Niemann-Pick type C

Glycosphingolipid

Glycosphingoid bases

Mouse models

LC-MS/MS

ABSTRACT

In lysosomal glycosphingolipid storage disorders, marked elevations in corresponding glycosphingoid bases (lyso-glycosphingolipids) have been reported, such as galactosylsphingosine in Krabbe disease, glucosylsphingosine in Gaucher disease and globotriaosylsphingosine in Fabry disease. Using LC-MS/MS, we comparatively investigated the occurrence of abnormal lyso-glycosphingolipids in tissues and plasma of mice with deficiencies in lysosomal α -galactosidase A, glucocerebrosidase and galactocerebrosidase. The nature and specificity of lyso-glycosphingolipid abnormalities are reported and compared to that in correspondingly more abundant N-acylated glycosphingolipids. Specific elevations in tissue and plasma globotriaosylsphingosine were detected in α -galactosidase A-deficient mice; glucosylsphingosine in glucocerebrosidase-deficient mice and galactosylsphingosine in galactocerebrosidase-deficient animals. A similar investigation was conducted for two mouse models of Niemann Pick type C (*Npc1^{tmh}* and *Npc1^{nmf164}*), revealing significant tissue elevation of several neutral glycosphingolipids and concomitant increased plasma glucosylsphingosine. This latter finding was recapitulated by analysis of plasma of NPC patients. The value of plasma glucosylsphingosine in biochemical confirmation of the diagnosis of NPC is discussed.

© 2016 Elsevier Inc. All rights reserved.

1. Introduction

The existence of glycosphingolipids (GSLs), membrane constituents consisting of a ceramide core with attached (oligo)saccharides, was demonstrated by Thudichum in the late 19th century through his pioneering studies on the chemical composition of the brain [1]. During the last century an increasing number of inherited disorders with characteristic accumulation of specific GSLs were described. It was later discovered that these glycosphingolipidoses result from inherited impairments in lysosomal degradation of GSLs (reviewed in reference [2]). In most cases the primary genetic defect concerns a lysosomal

glycosidase and examples of such enzymopathies are Tay-Sachs disease, GM1 gangliosidosis, Sandhoff disease, Fabry disease (FD), Gaucher disease (GD) and Krabbe disease [2]. Intralysosomal GSL accumulation may also arise secondarily as in the case of Niemann-Pick type C (NPC), in which cholesterol export from lysosomes is primarily impaired due to inherited defects in the non-enzymatic proteins NPC1 or NPC2 [3,4]. As firstly demonstrated for Krabbe disease, lysosomal storage of GSL can be accompanied by elevations in the corresponding glycosphingoid base (lyso-GSL) lacking the fatty acid, normally linked via an amide-bond to the sphingosine moiety [5]. For a schematic overview of relevant GSL metabolism see Supplemental Fig. 1. Due to difficulties in their quantitative detection, lyso-GSLs received relatively little attention for a long time. The recent use of LC-MS/MS in quantification of lyso-GSLs has revolutionized their analysis and led to a rapidly increasing amount of information on these compounds in health and disease. It has become apparent that elevations in these lipids occur in several lysosomal glycosphingolipidoses and that these can be exploited for diagnostic purposes [6]. Lyso-GSLs are more amphiphilic and water

Abbreviations: GSL, glycosphingolipid; Lyso-GSL, glycosphingoid base; Lyso-Gb3, globotriaosylsphingosine; G1cSph, glucosylsphingosine; GlySph, glucosylsphingosine; GlyCer, glycosylceramide.

* Corresponding author at: Leiden Institute of Chemistry, Gorlaeus Laboratories, Room number 0.3.15, Einsteinweg 55, 2333, CC, Leiden, The Netherlands.

E-mail address: j.m.f.g.aerts@lic.leidenuniv.nl (J.M. Aerts).

¹ These authors contributed equally to this work.

<http://dx.doi.org/10.1016/j.ymgme.2015.12.006>
1096-7192/© 2016 Elsevier Inc. All rights reserved.

soluble than their acylated (membrane lipid) counterparts, explaining their presence in the circulation and in urine. In patients suffering from the lysosomal disorders FD and GD, marked increases in globotriaosylsphingosine (lysoGb3) and glucosylsphingosine (GlcSph), respectively, are demonstrable in plasma as well as in urine [7–11].

To assess the specificity of abnormalities in lyso-GSLs, we comparatively determined the concentrations of GlcSph and lysoGb3, and corresponding GSLs, in the context of primary deficiencies in lysosomal glycosidases involved in GSL catabolism as well as in the context of a more generalized lysosomal dysfunction as in NPC. We investigated Twitcher mice deficient in galactocerebrosidase (GALC, EC 3.2.1.46), a model for Krabbe disease [12,13]; mice lacking LIMP-2, deficient in lysosomal glucocerebrosidase (GBA, EC 3.2.1.45) due to anomalous targeting of the enzyme to lysosomes, a model for Action Myoclonus Renal Failure syndrome (AMRF) [14,15]; genetically modified mice with an inducible GBA deficiency in the white blood cell lineage, a model for type 1 GD [16]; and mice deficient in α -galactosidase A (GLA, EC 3.2.1.22) due to the knock out of the GLA gene, a model for classic FD [17]. Additionally, we investigated two mouse models of NPC disease: the *Npc1^{nth}* mouse characterized by a null allele due to an early truncation of the NPC1 protein and mimicking the severe early infantile form of the disease [18], and the *Npc1^{nmf164}* mouse expressing NPC1 protein with a point mutation leading to partial loss of the protein's functionality and a more benign phenotype [19]. In our study we employed LC–MS/MS and internal ¹³C₅-isotope labeled lyso-GSLs standards for the sensitive quantification of these structures [10,20,21]. We here report on the characteristic abnormalities in lyso-GSLs in the various lysosomal storage disorders (LSDs) mouse models studied. The significance for human disease is illustrated by the demonstration of increased GlcSph in plasma of NPC patients.

2. Materials and methods

2.1. Animals

The generation of the GD1 mouse model (*Gba^{tm1Karl/tm1Karl}Tg(Mx1-cre)1Cgn/0*) with inducible knock down of GBA in the white blood cell lineage has been described previously [16,22]. These mice were maintained in individually ventilated cages with *ad libitum* food and water at the animal facility in Lund University Biomedical Center. Breeding and experimental procedures were approved by the Committee for Animal Ethics in Malmö/Lund, Sweden. Male *Fabry Gla^{-f0}* mice and wild-type (*wt*) littermates were generated by crossing heterozygous *Gla^{+/-}* female mice with *wt* males. Pups were genotyped as previously described [17]. *Gla^{tm1Kul}* (stock number 003535) and *Ldl^{tm1Her}* (stock number 002207) were purchased from The Jackson Laboratory (Bar Harbor, USA). *Npc1^{nih/nih}* and mice *Npc1^{nmf164}*, along with *wt* littermates (*Npc1^{+/+}*), were generated by crossing *Npc1^{+/nih}* or *Npc1^{+/nmf164}* males and females in-house. The heterozygous BALB/c Nctcr-*Npc1^{nm1N}*/J mice (stock number 003092) and C57BL/6J-*Npc1^{nmf164}*/J (stock number 004817) were obtained from The Jackson Laboratory (Bar Harbor, USA). Mouse pups were genotyped according to published protocols [18,19]. Breeding pairs of LIMP2 deficient mice were kindly provided by Prof. Paul Saftig (Kiel, Germany). Homozygous *wt* animals (*Limp2^{+/+}*) and homozygous knockout animals (*Limp2^{-/-}*) were generated by crossing heterozygous (*Limp2^{+/-}*) mice. Genotype was determined by PCR using genomic DNA [15]. Twitcher mice (*twi/twi*) along with *wt* littermates were generated by crossing heterozygous (*+/twi*) mice in-house. The heterozygous C57BL/6J B6.CE-*Galc^{twi}*/J mice (stock number 000845) were obtained from The Jackson Laboratory (Bar Harbor, USA). Mouse pups were genotyped as previously described [13]. Mice (3 weeks old) received the rodent AM-II diet (Arie Blok Diervoeders, Woerden, The Netherlands). LDLr deficient and Fabry mice in the cross-in study were fed a western-type of diet (casein 20%, cacao butter 15%, corn oil 1%, cholesterol 0.25%; Code: 4021.06, Arie Blok Diervoeders, Woerden, The Netherlands) for four weeks. The mice

were housed at the Institute Animal Core Facility in a temperature- and humidity-controlled room with a 12-h light/dark cycle and given free access to food and water *ad libitum*. All animal protocols were approved by the Institutional Animal Welfare Committee of the Academic Medical Center of Amsterdam in The Netherlands (DBC3021, DBC101698, DBC102873, DBC100757-125 and DBC17AC). All animal studies were performed in accordance with the European Communities Council Directive of 24 November 1986 (86/609/EEC). Mice were sacrificed at indicated age according to protocol, being first anesthetized with a dose of Hypnorm (0.315 mg/mL phenyl citrate and 10 mg/mL fluanisone) and Dormicum (5 mg/mL midazolam) according to their weight. The administered dose was 80 μ L/10 g bodyweight. Anesthetized animals were sacrificed by cervical dislocation. Organs were collected by surgery and rinsed with PBS. All samples and tissues collected were stored at -80°C prior to further analysis. Later, homogenates for lipid analysis were prepared, in 25 mM potassium phosphate buffer, pH 6.5, supplemented with 0.1% (v/v) Triton X-100 and protease inhibitors, using a tissue homogenizer (FastPrep®24).

2.2. Lipid measurements

GSLs and lyso-GSLs bases were measured with small modifications to earlier described methods [10,21,23]. Briefly, following extraction from biological samples neutral GSLs (ceramide, glucosylceramide, lactosylceramide and globotriaosylceramide) were determined by an HPLC-based procedure following microwave-assisted de-acylation of lipids and derivatization with *o*-phthalaldehyde [23]. The lyso-GSLs lysoGb3 and GlcSph were quantified with specific LC–MS/MS methods employing appropriate internal (isotope labeled) standards [10,21]. Lipid levels are expressed per gram of wet weight in the case of tissues or per mL in the case of plasma.

2.3. Glycosphingolipid digestion

The methods used to quantify GSLs and lyso-GSLs do not allow distinction between lipids differing only in terminal glucose or galactose moiety as those are incompletely separated by reverse-phase chromatography. Therefore we refer to the lipid species as glycosylated (gly) whenever the exact identity is not established. When mentioned, lipid samples were digested with recombinant GBA (rGBA, Cerezyme, Genzyme) to determine the percentage of glucosylated lipid species. For digestion 5 μ L of pure rGBA solution was mixed in 200 μ L of Mcllvaine buffer 150 mM pH 5.2 and used to dissolve the dried lipid pellet and incubated overnight at 37°C .

2.4. Patients

EDTA plasma samples of 17 NPC patients and 9 NPC carriers were collected prior to therapy at the Unidad de Investigación Translacional in Zaragoza. The status of affected or carrier of NPC disease was determined after the exonic sequencing of NPC1 and NPC2 genes. Filipin stainings of fibroblasts were conducted to complete the diagnosis. Plasma samples of 37 male and 42 female control subjects were collected at the Academic Medical Center according to protocol. Plasma samples were stored frozen at -20°C until further use.

2.5. Ethics statement

A written informed consent was obtained from each patient or their guardian. The study protocol was approved by the Ethics Committee for Clinical Investigation of Aragon (CEICA) in Spain. A written informed consent was also obtained from each healthy volunteer. The study was carried out in accordance with the ethical standards of the Declaration of Helsinki.

3. Results

3.1. Abnormalities in tissues of LSD mouse models

The concentrations of GSLs (ceramide [Cer], glycosylceramide [GlyCer], lactosylceramide [LacCer] and globotriaosylceramide [Gb3]) and of the lyso-GSLs (glycosylsphingosine (GlySph) and lysoGb3) were firstly determined for liver (Table 1) and spleen (Table 2) of male Fabry (*Gla*^{-f0}) mice, inducible Gaucher mice (*Gba*^{tm1Karl/tm1Karl}Tg(Mx1-cre)1Cgn/0), GBA-deficient *Limp2*^{-/-} and Krabbe (*Galc*^{-/-}) mice. As reference values, the same measurements were performed in wt mice with different backgrounds (BALB/c (Bc) and C57BL/6 (B6)) and included in the tables presented here. For statistical and fold difference analysis the mice were compared to the respective wt age-matched littermates.

The male FD mice, completely deficient in α -galactosidase A activity, show elevated hepatic and splenic Gb3 (15-fold and 35-fold, respectively), a finding not made for the other LSD models studied (Tables 1 & 2). Likewise, lysoGb3 is very clearly and specifically elevated in both tissues of FD mice: 430-fold in liver and 2200-fold increased in spleen (Tables 1 & 2). No significant changes in any of the other examined sphingolipids and sphingoid bases were detected in FD mice. In contrast, GBA-deficient *Limp2*^{-/-} mice show near normal GlyCer in combination with elevated GlySph in both tissues (Tables 1 & 2). Inducible GD type 1 (GD1, *Gba*^{tm1Karl/tm1Karl}Tg(Mx1-cre)1Cgn/0) mice present a 10–20 fold larger accumulation of both GlyCer and GlySph than the GBA-deficient *Limp2*^{-/-} animals. Of note, the GlyCer and GlcSph levels in GD1 mice varied considerably between animals, likely due to individual differences in induction of GBA knock down. *Galc*^{-/-} mice at end-stage show a marked elevation in GlySph in liver and spleen (Tables 1 & 2). *In vitro* digestion of GlySph with rGBA revealed that in both tissues only 10% is GlcSph and the remainder is most likely galactosylsphingosine (GalSph), also known as psychosine. No prominent increase in GlyCer was observed in the GALC-deficient liver and spleen, likely due to the fact that the majority of GlyCer in these organs is GlcCer.

Next, we analyzed liver and spleen of NPC – *Npc1*^{nmf164} and *Npc1*^{nmf164} – mice. *Npc1*^{nmf} animals are known to have a partial secondary deficiency in GBA and acid sphingomyelinase [24,25]. We report for the first time that GBA activity is also reduced in *Npc1*^{nmf164} mice (see Supplemental Fig. 2). We used materials from NPC mice sacrificed at end-stage, when the characteristic prominent increases in lysosomal cholesterol in tissues occur (Marques et al. unpublished). Both GlyCer and GlySph were found to be extremely elevated in liver and spleen of both NPC models, comparably to inducible GD1 mice (Tables 1 & 2). Digestion with rGBA showed that the vast majority (>95%) of GlyCer is GlcCer and that of GlySph is GlcSph (not shown). More modest, but highly significant, increases in LacCer, Gb3 and Cer levels were also observed in the liver and spleen of both NPC models.

3.2. Abnormalities in heart and kidney of Fabry mice

We investigated in more detail male FD mice by analysis of lipids in their heart and kidney, two affected organs in the disease (Table 3).

Corresponding wt littermates, also sacrificed at 20 weeks of age, were analyzed. As observed in liver and spleen, FD mouse heart and kidney show a clear increase of Gb3 in combination with a prominent elevation of lysoGb3 concentration. The FD heart accumulates more Gb3 (~20-fold increase compared to wt) than the kidneys (~5-fold increase compared to wt), while the FD kidneys store more lysoGb3 (~200-fold increase compared to wt) than the heart (~120-fold increase compared to wt) (Table 3).

3.3. Abnormalities in the plasma of LSD mouse models

We then compared the levels of lipids in plasma samples obtained from the various disease models (Table 4). None of the quantified glycosphingolipids (Cer, GlyCer, LacCer and Gb3) was significantly increased in any of the examined murine LSD models, except for a significant ~17-fold increased Gb3 in FD mice plasma. In sharp contrast, marked abnormalities were detected in plasma concentrations of lyso-GSLs in the LSD models. For instance, plasma of male FD mice showed ~200-fold elevated lysoGb3. In the case of GBA-deficient *Limp2*^{-/-} mice, plasma GlySph was 4-fold increased, but no clear abnormalities in other lyso-GSLs are detected. Insufficient plasma of GD1 mice was available for complete lipid analysis following that of GlcSph which was found to be 170-fold elevated [26]. In the case of Krabbe mice, plasma galactosylsphingosine (GalSph, more than 90% of total GlySph) was about ~12-fold increased, but other lyso-GSLs appeared normal. Whilst in the lysosomal enzymopathy models elevations in lyso-GSLs coincided with the primary GSL substrate, the picture for plasma of both NPC mouse models is different. In these animals a significant (2–4 fold) increase in plasma GlySph levels was observed in conjunction with significantly reduced lysoGb3 levels compared to age-matched wt controls (Table 4). Of note, the abnormality in plasma GlySph matches that observed in *Limp2*^{-/-} mice deficient in lysosomal GBA. The specificity of plasma lyso-GSLs abnormalities is also illustrated in Fig. 1 showing the relative increase in plasma GlySph and lysoGb3 in the various LSD murine models.

3.4. Source of elevated lysoGb3 in tissues of Fabry mice

The origin of the increased lysoGb3 in Fabry mouse tissues is unclear since we cannot discriminate *a priori* between endogenous production in a tissue, uptake of elevated lysoGb3 from the circulation or active formation of lysoGb3 from endocytosed lipoprotein-associated Gb3. To distinguish between these possibilities we exacerbated GSL stress from the circulation. For this purpose, FD mice were crossed with *Ldlr*^{-/-} mice showing impaired uptake of GSL-rich lipoprotein LDL and therefore very high plasma GSL levels when fed a lipid-rich western-type diet [27]. As shown in Fig. 2, male double-knockout *Gla*^{-f0}/*Ldlr*^{-/-} mice on a western-type diet show elevated GSL levels in their plasma. For example, plasma Gb3 in the *Gla*^{-f0}/*Ldlr*^{-/-} mice is even 3.5-fold higher compared to regular *Gla*^{-f0} FD mice that already show a 2.5-fold increase compared to *Ldlr*^{-/-} mice (Fig. 2). Similar observations were made for lysoGb3, being 3-fold increased in male

Table 1

Overview of the concentrations of major GSLs and lyso-GSLs in liver of various mouse LSD models. Indicated is the age at which the animals were sacrificed and the concentration of GSLs (nmol/g wet weight) and lyso-GSLs (pmol/g wet weight) in the liver. As reference wt mice of the BALB/c (Bc) and C57BL/6 (B6) background are shown. Data represent the mean \pm S.D. (n = 3–6).

Model	Wt B6	Wt Bc	Fabry	GD1	<i>Limp2</i> ^{-/-}	<i>Galc</i> ^{-/-}	<i>Npc1</i> ^{nmf}	<i>Npc1</i> ^{nmf}
Age (wk)	16	12	20	10–12	16	5	12	16
GlySph	13.33 \pm 5.77	15.13 \pm 1.03	24.17 \pm 0.90	4111.8 \pm 5106.7	254.30 \pm 139.84	402.20 \pm 6.84	3121.2 \pm 453.4	4786.0 \pm 1735.0
LysoGb3	14.23 \pm 1.45	7.46 \pm 0.71	7868.4 \pm 2817.6	14.75 \pm 1.81	5.58 \pm 3.10	11.17 \pm 1.46	13.56 \pm 0.85	20.46 \pm 3.07
GlyCer	33.1 \pm 3.2	34.2 \pm 5.2	38.7 \pm 3.9	289.4 \pm 465.6	23.4 \pm 13.0	35.7 \pm 9.7	419.4 \pm 147.0	354.5 \pm 80.7
Gb3	2.2 \pm 0.5	1.8 \pm 0.9	352.7 \pm 125.8	1.1 \pm 0.5	4.0 \pm 3.3	1.7 \pm 0.2	12.9 \pm 4.3	18.4 \pm 1.7
LacCer	14.2 \pm 1.4	29.5 \pm 9.9	11.3 \pm 1.3	5.0 \pm 3.2	5.8 \pm 2.6	7.0 \pm 1.6	248.6 \pm 73.3	170.4 \pm 26.2
Cer	150.0 \pm 4.0	338.1 \pm 93.4	384.4 \pm 29.8	91.9 \pm 21.7	111.5 \pm 40.9	134.5 \pm 4.3	633.4 \pm 203.3	438.7 \pm 44.7

Table 2
Overview of the concentrations of major GSLs and lyso-GSLs in spleen of various mouse LSD models. Indicated is the age at which the animals were sacrificed and the concentration of GSLs (nmol/g wet weight) and lyso-GSLs (pmol/g wet weight) in the spleen. As reference wt mice of the BALB/c (Bc) and C57BL/6 (B6) background are shown. Data represent the mean \pm S.D. (n = 3–6).

Model	Wt B6	Wt Bc	Fabry	GD1	<i>Limp2</i> ^{−/−}	<i>Galc</i> ^{−/−}	<i>Npc1</i> ^{nlh}	<i>Npc1</i> ^{nmf}
Age (wk)	16	12	20	10–12	16	5	12	16
GlySph	23.3 \pm 5.77	35.7 \pm 14.6	60.28 \pm 23.93	17,532.5 \pm 9023.9	399.98 \pm 143.72	254.10 \pm 28.36	1719.9 \pm 222.6	1682.0 \pm 262.0
LysoGb3	6.20 \pm 1.38	4.69 \pm 2.1	11,157.3 \pm 5664.9	6.88 \pm 1.33	1.70 \pm 0.34	2.53 \pm 1.03	30.17 \pm 2.40	27.18 \pm 5.41
GlyCer	133.1 \pm 11.9	89.1 \pm 9.2	381.9 \pm 30.7	1030.0 \pm 1397.5	73.8 \pm 6.6	132.0 \pm 6.1	348.0 \pm 83.2	336.5 \pm 41.7
Gb3	46.2 \pm 5.8	51.0 \pm 4.4	1417.9 \pm 245.6	24.9 \pm 9.3	9.8 \pm 5.5	43.0 \pm 3.5	85.5 \pm 26.4	83.8 \pm 12.9
LacCer	17.7 \pm 1.4	13.3 \pm 3.5	40.9 \pm 42.2	13.3 \pm 2.6	6.1 \pm 2.0	13.2 \pm 0.9	164.0 \pm 40.0	116.5 \pm 17.3
Cer	104.6 \pm 8.5	71.6 \pm 3.8	125.4 \pm 13.8	99.5 \pm 16.7	70.1 \pm 6.5	89.0 \pm 7.2	161.1 \pm 15.4	205.9 \pm 13.4

Gla^{−/0}/*Ldlr*^{−/−} mice as compared to *Gla*^{−/0} FD mice that present 95-fold as compared to *Ldlr*^{−/−} mice (Fig. 2).

Analysis of tissues revealed that despite the extremely high plasma Gb3 and lysoGb3 in male *Gla*^{−/0}/*Ldlr*^{−/−} mice, the concentration of Gb3 or lysoGb3, was similar in their liver, spleen, heart and kidney to that of regular male Fabry mice (see Fig. 2 and Supplemental Fig. 3). Apparently, the chronic exposure to high levels of circulating lyso-GSLs contributed little to the accumulation of the same lipids in the various tissues analyzed, suggesting that these have largely an endogenous production.

3.5. Accumulation of sphingoid bases in Niemann–Pick type C patients

The findings made with the murine LSD models are recapitulated by analysis of plasma samples from patients suffering from FD, GD and AMRF. We previously documented that plasma lysoGb3 is 200-fold increased in male classic FD patients [21,28]. Likewise, plasma GlcSph has been found to be on average 300-fold increased in patients suffering from GD1 [8,10]. Finally, in the two AMRF patients examined, plasma GlySph was found to be 8-fold elevated [29]. These findings prompted us to comparatively examine plasma obtained from NPC patients.

The plasma concentrations of Cer, LacCer, and Gb3 were not significantly abnormal in NPC patients (n = 17, median age = 42, range 2–68 years) or carriers for the disease (n = 9, age = 53, range 28–59 years) compared to healthy control individuals (n = 79, age = 38, range 20–65 years). Of note, plasma GlyCer in the NPC patients showed a trend of minor elevation, however the difference with normal subjects did not reach significance. As in the mouse models, analysis of lyso-GSLs did reveal much clearer differences between NPC patients and healthy subjects. Plasma lysoGb3 in NPC patients (mean 0.34, range 0.23–0.54 pmol/mL) was within the lower range of the controls (mean 0.39, range 0.22–0.64 pmol/mL, Fig. 3). A significant difference was observed for plasma GlySph, being on average higher in NPC patients (mean 1.76, range 0.72–4.49 pmol/mL) with some overlap with the upper control range (mean 0.78, range 0.15–2.50 pmol/mL).

Oxysterols have been documented as a sensitive biomarker for NPC [30]. To compare the noted abnormality in plasma GlySph, oxysterols

were determined in the same plasma samples. Plasma oxysterols were found to be increased (mean 343, range 34–1157 ng/mL) compared to controls (<102.8 ng/mL) [31]. The abnormality of plasma oxysterols in the patients was more prominent than the deviation in GlySph levels. However, no correlation was observed between incremental oxysterols and GlySph in NPC patients (Fig. 4).

4. Discussion

Our comparative quantitative investigation of GSLs and corresponding lyso-GSLs in mouse models of deficiencies of α -galactosidase A, GBA and GALC recapitulates earlier observations in patients suffering from FD, GD1/AMRF and Krabbe disease, respectively [7,22,29,32]. The noted abnormalities in GSLs and lyso-GSLs and their specificity for the various disorders merit discussion.

As in male patients, deficiency of α -galactosidase A in male mice leads to increased levels of the primary substrate Gb3 in several tissues such as liver (15-fold), spleen (35-fold), heart (20-fold) and kidney (5-fold). Gb3 is also considerably elevated in plasma (30-fold). A far more striking abnormality is seen for the lyso-GSL of Gb3, lysoGb3. In plasma of Fabry mice lysoGb3 exceeds normal levels 190-fold. LysoGb3 concentrations are increased 430-fold in liver, 2200-fold in the spleen, 120-fold in heart and 200-fold in kidney. The very high lysoGb3 levels of spleen are likely explained by the high rate of degradation by splenic macrophages of senescent blood cells rich in globosides. Earlier we observed that lipid-laden macrophages occur in Fabry patients as reflected by increased plasma chitotriosidase [33]. Of interest, sphingolipid abnormalities in this animal model are restricted to Gb3 and lysoGb3. No abnormalities are demonstrable for GlyCer, LacCer or ceramide. Likewise, GlySph is normal in the investigated Fabry animals. Of note, GlcCer is not decreased in Fabry mice suggesting that there is no feedback on GSL biosynthesis to avoid ongoing Gb3 accumulation.

FD is a complex multi-organ disease with broad clinical manifestations such as cardiomyopathy, renal failure, pain and peripheral neuropathy [34]. We, and others, looked for correlations between plasma lysoGb3 levels and various disease manifestations. Although patients with higher lysoGb3 levels showed a trend to more pronounced disease manifestations, no significant correlation of plasma lysoGb3 and specific symptoms was noted except for pain [35,36]. Very recently Choi and colleagues presented experimental evidence for a direct effect of lysoGb3 on sensory neurons [37]. It was reported that plantar administration of lysoGb3 induces mechanical allodynia in mice. Sensory neurons expressing nociceptor markers showed enhanced peak current densities of voltage-dependent Ca²⁺ channels in the presence of 1 μ M lysoGb3, close to concentrations occurring in plasma of male FD patients [7]. The authors concluded that lysoGb3 plays a direct role in the sensitization of peripheral nociceptive neurons. At present a direct role for lysoGb3 in the pathophysiology of heart and kidney in Fabry patients has not been demonstrated. Noteworthy however, in connection to renal disease, is the demonstration of pro-fibrotic action of lysoGb3 in experimental models [38,39].

Our findings regarding lyso-GSLs and lipids in the mouse models of GBA deficiency are consistent with reports for Gaucher patients and

Table 3
Overview of the concentrations of major GSLs and lyso-GSLs in heart and kidney of FD mouse model.

Fabry male mice and wt littermates were sacrificed at 20 weeks of age. The concentration of GSLs and lyso-GSLs in the kidney and heart is expressed in nmol/g wet weight and pmol/g wet weight, respectively. Data represent the mean \pm S.D. (n = 3).

Organ	Heart		Kidney	
Model	Wt	Fabry	Wt	Fabry
GlySph	3.7 \pm 3.1	1.2 \pm 2.1	33.6 \pm 4.4	26.2 \pm 1.5
LysoGb3	4.2 \pm 0.8	496.83 \pm 87.3	8.1 \pm 3.1	1568.3 \pm 76.6
GlyCer	108.2 \pm 38.7	97.4 \pm 12.4	51.5 \pm 5.4	54.4 \pm 0.3
Gb3	60.7 \pm 3.7	1173.4 \pm 109.8	114.3 \pm 32.0	559.8 \pm 58.5
LacCer	Trace ^a	Trace ^a	7.5 \pm 0.6	15.7 \pm 1.6
Cer	118.9 \pm 7.8	118.1 \pm 4.8	250.7 \pm 3.7	296.2 \pm 17.4

^a Discernable signal but below limit of quantification (<10 \times noise).

Table 4

Overview of the concentrations of major GSLs and lyso-GSLs in plasma of various mouse LSD models. Indicated is the age at which the animals were sacrificed and the concentration of the lipids in plasma in nmol/mL and those of lyso-GSLs in pmol/mL. As reference wt mice of the BALB/c (Bc) and C57BL/6 (B6) background are shown. Data represent the mean \pm S.D. (n = 3–5).

Model	Wt B6	Wt Bc	Fabry	GD1 [26]	<i>Limp2</i> ^{−/−}	<i>Galc</i> ^{−/−}	<i>Npc1</i> ^{nh}	<i>Npc1</i> ^{nmf}
Age (wk)	16	12	20	20–68	16	5	12	16
GlySph	0.89 \pm 0.09	0.50 \pm 0.07	0.16 \pm 0.11	65.88 \pm 38.69	3.56 \pm 1.73	11.83 \pm 1.01	1.56 \pm 0.62	4.04 \pm 0.57
LysoGb3	1.21 \pm 0.36	0.69 \pm 0.13	571.15 \pm 22.91	N.A.	0.90 \pm 0.66	0.67 \pm 0.49	0.15 \pm 0.03	0.33 \pm 0.17
GlyCer	3.05 \pm 0.55	1.94 \pm 0.18	3.14 \pm 0.01	4.30 \pm 1.87	1.80 \pm 1.08	2.41 \pm 0.39	1.73 \pm 0.53	2.79 \pm 0.92
Gb3	0.24 \pm 0.02	0.28 \pm 0.04	4.11 \pm 0.01	N.A.	0.42 \pm 0.28	Trace ^a	0.14 \pm 0.05	0.18 \pm 0.02
LacCer	0.19 \pm 0.04	0.27 \pm 0.05	Trace ^a	N.A.	0.34 \pm 0.26	Trace ^a	0.30 \pm 0.04	0.17 \pm 0.01
Cer	2.15 \pm 0.54	2.43 \pm 0.51	2.21 \pm 0.01	2.97 \pm 1.35	1.22 \pm 0.33	1.36 \pm 0.12	2.13 \pm 0.56	1.59 \pm 0.19

^a Discernable signal but below limit of quantification (<10 \times noise). N.A. – not available.

AMRF patients on this matter [8,11,29,40]. It is of interest to point out the differences noted between mice with induced GBA knock-down in white blood cells and mice lacking LIMP2, the transporter of GBA to lysosomes [15,16,22,41]. In the latter animals GBA is extremely low in most cell types, but not in macrophages likely due to re-uptake of faulty secreted GBA [29,42] (Gaspar et al. unpublished). Our findings with GBA-deficient *Limp2*^{−/−} mice suggest that most cell types despite major deficiency in GBA successfully prevent GlcCer accumulation and apparently their macrophages have sufficient residual GBA to limit GlcCer storage by transforming it to GlcSph. This however does not hold for GBA-deficient macrophages in GD1 mice. Here prominent GlcCer accumulation occurs, accompanied by elevated plasma GlcSph. Thus, in the GBA-deficient macrophages of Gaucher patients the loading of lysosomes with GSLs surpasses the capacity to re-route accumulating GlcCer to GlcSph. Another example of adaptation is presented by wt and Fabry mice in which deficiency of the LDL receptor is introduced. Both these animals develop upon high fat feeding very high plasma concentrations of various GSLs. The mice also show a modest increase in plasma GlcSph which might point to an adaptive attempt to prevent lysosomal GlcCer storage.

The increased tissue and plasma GlcSph levels in GBA-deficient *Limp2*^{−/−} mice suggest that in tissues GlcCer is actively deacylated to GlcSph, which subsequently reaches the circulation. Indeed, we earlier presented evidence that GBA-deficient cells upon pharmacological inhibition of GBA start to accumulate GlcCer and concomitantly form GlcSph [8], most likely due to the action of ASAH1 (Ferraz et al. unpublished). In experimental cell models GlcSph has been found to be potentially toxic by causing lysis of red blood cells, impairing cell fission during cytokinesis, damaging specific neurons, hampering growth, impairing osteoblasts, and promoting inflammation via activation of phospholipase A2 [43,44]. The concentrations of GlcSph required for the observed toxic effects exceed those measured in plasma of GD patients. Consequently, it remains unclear whether the GlcSph contributes to the symptoms observed in GD patients, such as occurrence of hemolysis, multinucleated macrophages, neuropathology, growth retardation, bone deterioration

and chronic low grade inflammation [6]. Recent investigations by Cox and coworkers have revealed an intriguing correlation between the occurrence of lymphoma in *Gba*^{tm1Kar/tm1Kar}Tg(Mx1-cre)1Cgn/0 mice and GlcSph levels [26,45]. Currently a direct role for elevated GlcSph in the symptomatology of GD has not yet been unequivocally demonstrated.

The noted elevation in plasma GalSph in galactocerebrosidase deficient Twitcher mice is similar to the reported elevation of GalSph in Krabbe patient materials [46]. A direct pathological role for GalSph has been proposed for the neuropathology of Krabbe disease. GalSph triggers apoptosis of oligodendrocytes and Schwann cells by disrupting lipid rafts in myelinating glia [47,48]. This results in demyelination affecting both the central and peripheral nervous systems [49,50]. However, there is still discussion whether axonopathy is secondary to demyelination or if is directly caused by the GalSph accumulation in Krabbe neurons [51].

Besides lysosomal enzymopathies, we included in our investigation NPC disease mice with a more generalized lysosomal dysfunction. The investigated *Npc1*^{nh} mouse strain is a spontaneous model of NPC disease. The animals present a null allele and are thus fully deficient in NPC1 protein [18,24]. This lysosomal transmembrane protein, together with the soluble NPC2 protein, is responsible for the efflux of free (unesterified) cholesterol from the late-endosomal/lysosomal compartment to the cytosol [52]. Deficiency in NPC1 protein leads to a massive accumulation of cholesterol in visceral organs of the mice. We and others have shown that, at end-stage, hepatic cholesterol levels are 10-fold higher in *Npc1*^{nh} mice compared to wt littermates [53,54] (Marques et al. unpublished). The extreme sterol accumulation in lysosomes is thought to impair the activity of other lysosomal hydrolases [24,25,55]. GBA activity, for example, is reduced to half in the liver of *Npc1*^{nh} mice [24] and *Npc1*^{nmf64} late-onset mice (see Supplemental Fig. 2) for reasons not fully elucidated yet. The deficient GBA activity in NPC lysosomes leads to a prominent accumulation of its glucosylated substrate: GlcCer. In fact, the observed accumulation of GlcCer in liver of both studied NPC mouse strains even surpasses levels detected in the livers of GD1 mice with an induced GBA deficiency in the white blood cell lineage (see Table 1). Concomitantly GlcSph is elevated in *Npc1*^{nh} livers, but to a lesser extent possibly due to partly impaired acid ceramidase activity. Increased levels of other sphingolipids such as Cer, LacCer and Gb3 also occur in liver of the studied *Npc1*^{nh} mice. As earlier observed by others [24,56], we noted elevated gangliosides in tissues of NPC mice (not shown). Accumulation of sphingomyelin in *Npc1*^{nh} liver has been extensively documented [24,54,56]. *Npc1*^{nmf64} mice present a milder course of NPC disease but at end-stage show similar lipid abnormalities as *Npc1*^{nh} mice.

Recently increased levels of GlcSph have been reported in NPC patient cohorts [57,58]. Our investigation confirms that the lyso-GSL tends to be elevated in the majority of patients analyzed. Recently, elevations in phosphorylcholine-sphingosine (deacylated sphingomyelin, lysoSM) and in the isoform lysoSM-509 were described in plasma of NPC patients [57,59]. Plasma oxysterols have earlier been validated as sensitive biomarker for NPC [30,60]. We measured in the same NPC

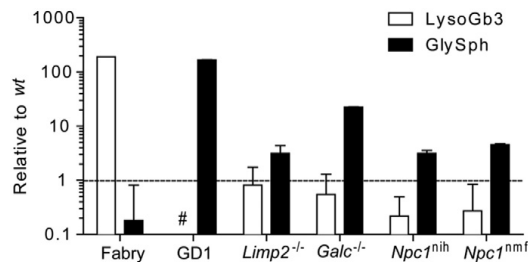


Fig. 1. Relative changes in lyso-GSLs in plasma of LSD mouse models. Levels of GlySph and lysoGb3 in the plasma of LSD mouse models relative to respective wt littermates. [#] Levels of lysoGb3 on plasma of GD1 mice are not available.

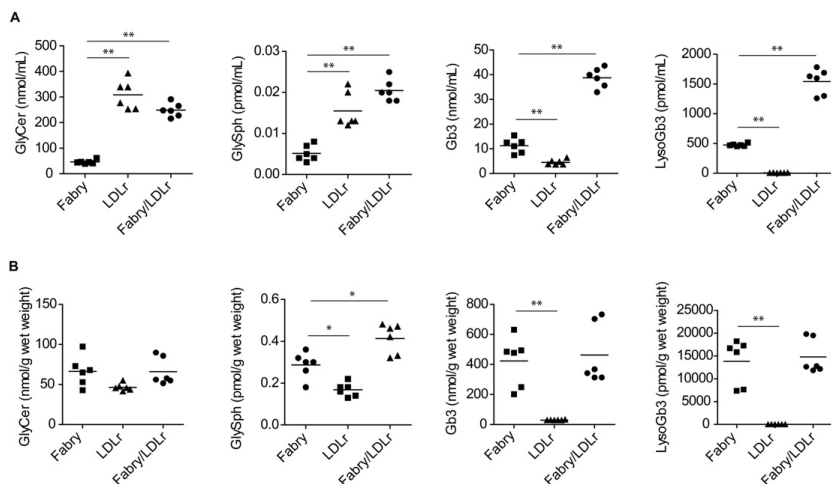


Fig. 2. LDLr deficiency in Fabry mice on a western-type diet exacerbates lipid abnormalities in plasma but not in liver. Upper panel: Plasma GSL (Gb3 and GlyCer) and lyso-GSL (lysoGb3 and GlySph) in male *Gla*⁻⁰ (Fabry), *Ldlr*^{-/-}, and combined *Gla*⁻⁰/*Ldlr*^{-/-} mice receiving western type diet. Lower panel: Liver lipid levels as above. Data were analyzed by Mann-Whitney u-test: * *P* < 0.05; ** *P* < 0.01.

plasma samples GlySph and oxysterol. Plasma oxysterol levels were found to be increased (mean 343, range 34–1157 ng/mL) as compared to controls (<102.8 ng/mL). The abnormality in plasma oxysterols in NPC patients was far more prominent than the one observed in GlySph and no correlation between the two was observed. From these findings it may be concluded that for confirmation of the NPC diagnosis demonstration of abnormal plasma oxysterols should be preferred over that of GlcSph.

In summary, our comparative LC-MS/MS-based analysis of GlySph and lysoGb3 in tissues and plasma of mouse LSD models with

deficiencies in GLA, GBA and GALC revealed specific abnormalities coinciding with the GSL substrate of the deficient glycosidases. Interestingly *Limp2*^{-/-} mice are an exception to this rule and seem to almost completely avoid GlcCer accumulation. In two distinct mouse models of NPC (*Npc1*^{hih} and *Npc1*^{nmf164}) accumulation of several neutral GSLs was observed in tissues and concomitantly elevations in plasma GlySph were detected. This finding was confirmed by the noted increase in GlySph in plasma of NPC patients. Our study points out that detection of lyso-GSLs may assist in diagnosis of glycosphingolipidoses, however care should be taken to establish the specificity of noted abnormalities

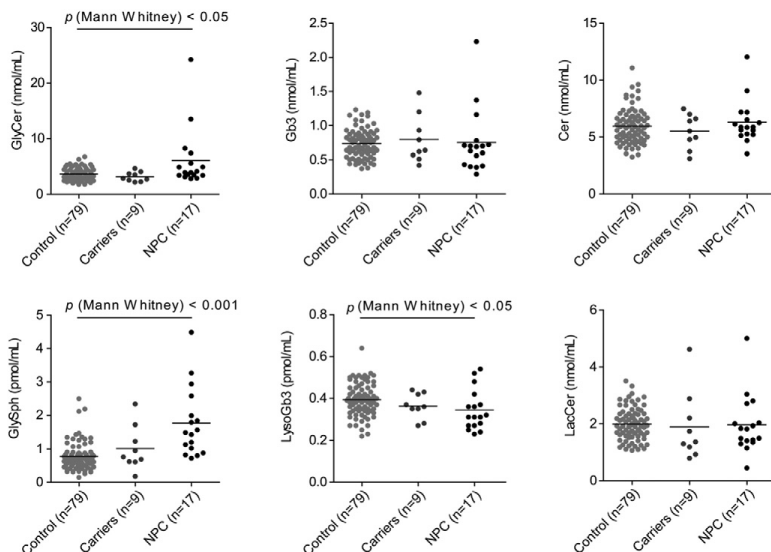


Fig. 3. GSLs and lyso-GSLs in NPC patients. Plasma levels of GSLs and lyso-GSLs in healthy volunteers (*n* = 79), carriers of one known mutation on the *Npc1* gene (*n* = 9) and confirmed NPC patients (*n* = 17). Data were analyzed using the Mann-Whitney u test.

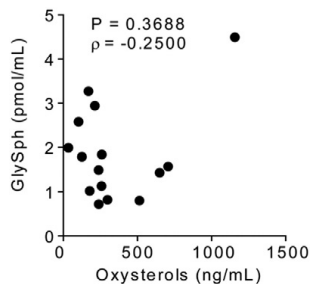


Fig. 4. Correlation between GlySph and Oxysterols plasma levels in diagnosed NPC patients.

by rigorous documentation of plasma lyso-GSL in other conditions with impaired lysosome function, for genetic reasons and possibly as well when induced by chronic exposure to lysosomotropic drugs.

Acknowledgments

We would like to thank Prof. Stefan Karlsson for providing the GBA mouse tissues and Prof. Paul Saftig for the *Limp2*^{-/-} mice used in this study. Johannes Aerts and Herman Overkleeft were funded by the ERC AdG CHEMBIOSPHIN (290836). Paulo Gaspar was funded by Fundação para a Ciência e Tecnologia (SFRH/BD/72862/2010).

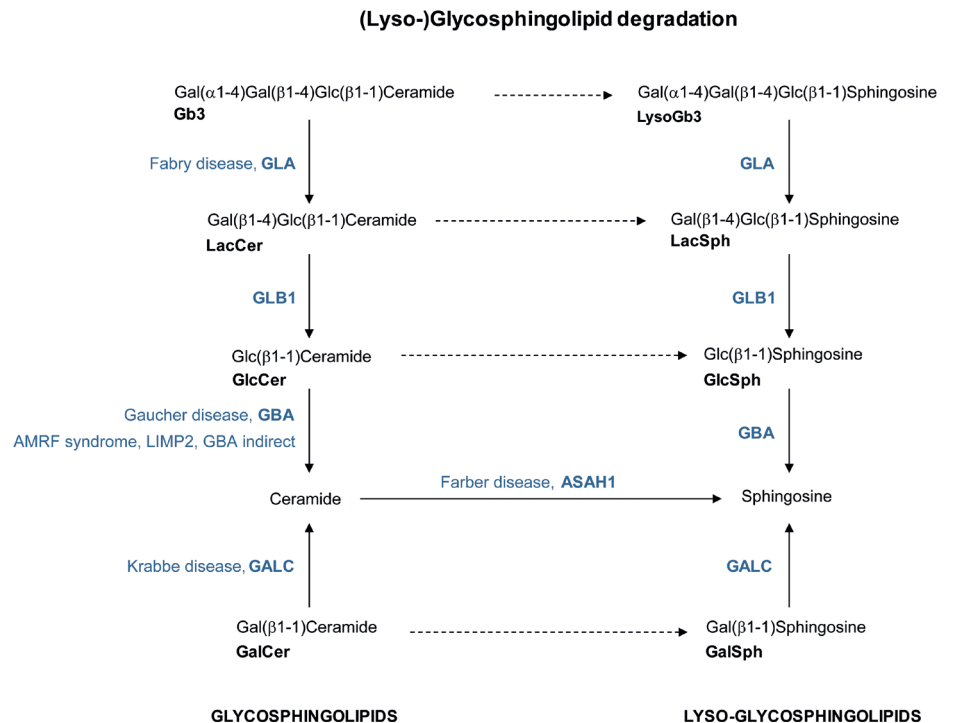
Appendix A. Supplementary data

Supplementary data to this article can be found online at <http://dx.doi.org/10.1016/j.yimgme.2015.12.006>.

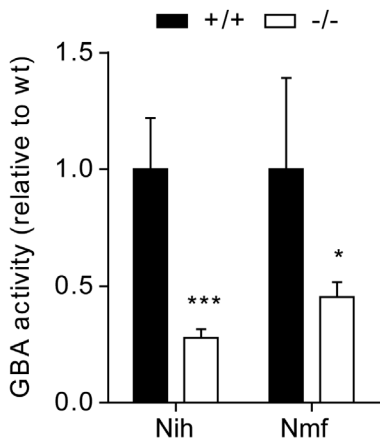
References

- [1] J. Thudichum, A Treatise on the Chemical Constitution of the Brain, Bailliere Tindall and Cox, London, 1884.
- [2] H. Schulze, K. Sandhoff, Sphingolipids and lysosomal pathologies, *Biochim. Biophys. Acta* 1841 (2014) 799–810.
- [3] E.D. Carstea, J.A. Morris, K.G. Coleman, S.K. Loftus, D. Zhang, C. Cummings, et al., Niemann–Pick C1 disease gene: homology to mediators of cholesterol homeostasis, *Science* 277 (1997) 228–231.
- [4] S. Naureckiene, D.E. Sleat, H. Lackland, A. Fensom, M.T. Vanier, R. Wattiaux, et al., Identification of HE1 as the second gene of Niemann–Pick C disease, *Science* 290 (2000) 2298–2301.
- [5] T. Miyatake, K. Suzuki, Additional deficiency of psychosine galactosidase in globoid cell leukodystrophy: an implication to enzyme replacement therapy, *Birth Defects Orig. Artic. Ser.* 9 (1973) 136–140.
- [6] M.J. Ferraz, W.W. Kallemeijn, M. Mirzaian, D. Herrera Moro, A. Marques, P. Wisse, et al., Gaucher disease and Fabry disease: new markers and insights in pathophysiology for two distinct glycosphingolipidoses, *Biochim. Biophys. Acta* 1841 (2014) 811–825.
- [7] J.M. Aerts, J.E. Groener, S. Kuiper, W.E. Donker-Koopman, A. Strijland, R. Ottenhoff, et al., Elevated globotriaosylsphingosine is a hallmark of Fabry disease, *Proc. Natl. Acad. Sci. U. S. A.* 105 (2008) 2812–2817.
- [8] N. Dekker, L. van Dussen, C.E.M. Hollak, H. Overkleeft, S. Scheij, K. Ghauharali, et al., Elevated plasma glucosylsphingosine in Gaucher disease: relation to phenotype, storage cell markers, and therapeutic response, *Blood* 118 (2011) e118–e127.
- [9] C. Aury-Blais, M. Boutin, R. Gagnon, F.O. Dupont, P. Lavoie, J.T.R. Clarke, Urinary globotriaosylsphingosine-related biomarkers for Fabry disease targeted by metabolomics, *Anal. Chem.* 84 (2012) 2745–2753.
- [10] M. Mirzaian, P. Wisse, M.J. Ferraz, H. Gold, W.E. Donker-Koopman, M. Verhoeck, et al., Mass spectrometric quantification of glucosylsphingosine in plasma and urine of type 1 Gaucher patients using an isotope standard, *Blood Cells Mol. Dis.* 54 (2015) 307–314.
- [11] A. Rölfs, A.-K. Giese, U. Grittner, D. Mascher, D. Elstein, A. Zimran, et al., Glucosylsphingosine is a highly sensitive and specific biomarker for primary diagnostic and follow-up monitoring in gaucher disease in a non-Jewish, Caucasian cohort of Gaucher disease patients, *PLoS One* 8 (2013), e79732.
- [12] K. Suzuki, The twitcher mouse. A model of human globoid cell leukodystrophy (Krabbe's disease), *Am. J. Pathol.* 111 (1983) 394–397.
- [13] N. Sakai, K. Inui, N. Tatsumi, H. Fukushima, T. Nishigaki, M. Taniike, et al., Molecular cloning and expression of cDNA for murine galactocerebrosidase and mutation analysis of the twitcher mouse, a model of Krabbe's disease, *J. Neurochem.* 66 (1996) 1118–1124.
- [14] S.F. Berkovic, L.M. Dibbens, A. Oshlack, J.D. Silver, M. Katerelos, D.F. Vears, et al., Array-based gene discovery with three unrelated subjects shows SCARB2/LIMP-2 deficiency causes myoclonus epilepsy and glomerulosclerosis, *Am. J. Hum. Genet.* 82 (2008) 673–684.
- [15] A.-C. Gamp, Y. Tanaka, R. Lüllmann-Rauch, D. Wittke, R. D'Hooge, P.P. De Deyn, et al., LIMP-2/LGP85 deficiency causes ureteric pelvic junction obstruction, deafness and peripheral neuropathy in mice, *Hum. Mol. Genet.* 12 (2003) 631–646.
- [16] I.B. Enquist, E. Nilsson, A. Ooka, J.-E. Månsson, K. Olsson, M. Ehinger, et al., Effective cell and gene therapy in a murine model of Gaucher disease, *Proc. Natl. Acad. Sci. U. S. A.* 103 (2006) 13819–13824.
- [17] T. Ohshima, G.J. Murray, W.D. Swaim, G. Longenecker, J.M. Quirk, C.O. Cardarelli, et al., Alpha-Galactosidase A deficient mice: a model of Fabry disease, *Proc. Natl. Acad. Sci. U. S. A.* 94 (1997) 2540–2544.
- [18] S.K. Loftus, J.A. Morris, E.D. Carstea, J.Z. Gu, C. Cummings, A. Brown, et al., Murine model of Niemann–Pick C disease: mutation in a cholesterol homeostasis gene, *Science* 277 (1997) 232–235.
- [19] R.A. Maue, R.W. Burgess, B. Wang, C.M. Wooley, K.L. Seburn, M.T. Vanier, et al., A novel mouse model of Niemann–Pick type C disease carrying a D1005G-Npc1 mutation comparable to commonly observed human mutations, *Hum. Mol. Genet.* 21 (2012) 730–750.
- [20] P. Wisse, H. Gold, M. Mirzaian, M.J. Ferraz, G. Lutteke, R.J.B.H.N. van den Berg, et al., Synthesis of a panel of carbon-13-labelled (glyco)sphingolipids, *Eur. J. Org. Chem.* (2015) 2661–2677.
- [21] H. Gold, M. Mirzaian, N. Dekker, M. Joao Ferraz, J. Lugtenburg, J.D.C. Codée, et al., Quantification of globotriaosylsphingosine in plasma and urine of fabry patients by stable isotope ultra-performance liquid chromatography–tandem mass spectrometry, *Clin. Chem.* 59 (2012) 1–10.
- [22] M. Dahl, A. Doyle, K. Olsson, J.-E. Månsson, A.R.A. Marques, M. Mirzaian, et al., Lentiviral gene therapy using cellular promoters cures type 1 Gaucher disease in mice, *Mol. Ther.* 23 (2015) 835–844.
- [23] J.E.M. Groener, B.J.H.M. Poorthuis, S. Kuiper, M.T.J. Helmond, C.E.M. Hollak, J.M.F.G. Aerts, HPLC for simultaneous quantification of total ceramide, glucosylceramide, and ceramide trihexoside concentrations in plasma, *Clin. Chem.* 53 (2007) 742–747.
- [24] P.G. Pentchev, A.E. Gal, A.D. Booth, F. Omodeo-Sale, J. Fouks, B.A. Neumeyer, et al., A lysosomal storage disorder in mice characterized by a dual deficiency of sphingomyelinase and glucocerebrosidase, *Biochim. Biophys. Acta* 619 (1980) 669–679.
- [25] R. Salvioli, S. Scarpa, F. Ciffloni, M. Tatti, C. Ramoni, M.T. Vanier, et al., Glucosylceramide mass and subcellular localization are modulated by cholesterol in Niemann–Pick disease type C, *J. Biol. Chem.* 279 (2004) 17674–17680.
- [26] E.V. Pavlova, J. Archer, S. Wang, N. Dekker, J.M. Aerts, S. Karlsson, et al., Inhibition of UDP-glucosylceramide synthase in mice prevents Gaucher disease-associated B-cell malignancy, *J. Pathol.* 235 (2015) 113–124.
- [27] E. Lombardo, C.P. van Roomen, G.H. van Puijvelde, R. Ottenhoff, M. van Eijk, J. Aten, et al., Correction of liver steatosis by a hydrophobic iminosugar modulating glycosphingolipids metabolism, *PLoS One* 7 (2012), e38520.
- [28] M.J. van Breemen, S.M. Rombach, N. Dekker, B.J. Poorthuis, G.E. Linthorst, A.H. Zwiderman, et al., Reduction of elevated plasma globotriaosylsphingosine in patients with classic Fabry disease following enzyme replacement therapy, *Biochim. Biophys. Acta* 1812 (2011) 70–76.
- [29] P. Gaspar, W.W. Kallemeijn, A. Strijland, S. Scheij, M. Van Eijk, J. Aten, et al., Action myoclonus-renal failure syndrome: diagnostic applications of activity-based probes and lipid analysis, *J. Lipid Res.* 55 (2014) 138–145.
- [30] X. Jiang, R. Sidhu, F.D. Porter, N.M. Yanjanin, A.O. Speak, D.T. de Vruete, et al., A sensitive and specific LC–MS/MS method for rapid diagnosis of Niemann–Pick C1 disease from human plasma, *J. Lipid Res.* 52 (2011) 1435–1445.
- [31] J.J. Cebolla, I. De Castro-Orós, P. Irún, P. Alfonso, L. López de Frutos, M. Andrade-Campos, et al., Experience with 7-ketocholesterol and ccl18/parc as surrogate biomarkers in a series of Spanish Niemann–Pick disease type C patients, *Mol. Genet. Metab.* 114 (2015) S29.
- [32] P.D. Whitfield, P.C. Sharp, R. Taylor, P. Meikle, Quantification of galactosylsphingosine in the twitcher mouse using electrospray ionization–tandem mass spectrometry, *J. Lipid Res.* 42 (2001) 2092–2095.
- [33] A.C. Vedder, J. Cox-Brinkman, C.E.M. Hollak, G.E. Linthorst, J.E.M. Groener, M.T.J. Helmond, et al., Plasma chitotriosidase in male Fabry patients: a marker for monitoring lipid-laden macrophages and their correction by enzyme replacement therapy, *Mol. Genet. Metab.* 89 (2006) 239–244.
- [34] D.P. Germain, Fabry disease, *Orphanet J. Rare Dis.* 5 (2010) 30.
- [35] S.M. Rombach, B. van den Bogaard, E. de Groot, J.E.M. Groener, B.J. Poorthuis, G.E. Linthorst, et al., Vascular aspects of Fabry disease in relation to clinical manifestations and elevations in plasma globotriaosylsphingosine, *Hypertension* 60 (2012) 998–1005.
- [36] M. Biegstraaten, G.E. Linthorst, I.N. van Schaik, C.E.M. Hollak, Fabry disease: a rare cause of neuropathic pain, *Curr. Pain Headache Rep.* 17 (2013) 365.
- [37] L. Choi, J. Vernon, O. Kopach, M.S. Minnett, K. Mills, P.T. Clayton, et al., The Fabry disease-associated lipid lyso-Gb3 enhances voltage-gated calcium currents in sensory neurons and causes pain, *Neurosci. Lett.* 594 (2015) 163–168.
- [38] M.D. Sanchez-Niño, A.B. Sanz, S. Carrasco, M.A. Saleem, P.W. Mathieson, J.M. Valdivielso, et al., Globotriaosylsphingosine actions on human glomerular podocytes: implications for Fabry nephropathy, *Nephrol. Dial. Transplant.* 26 (2011) 1797–1802.

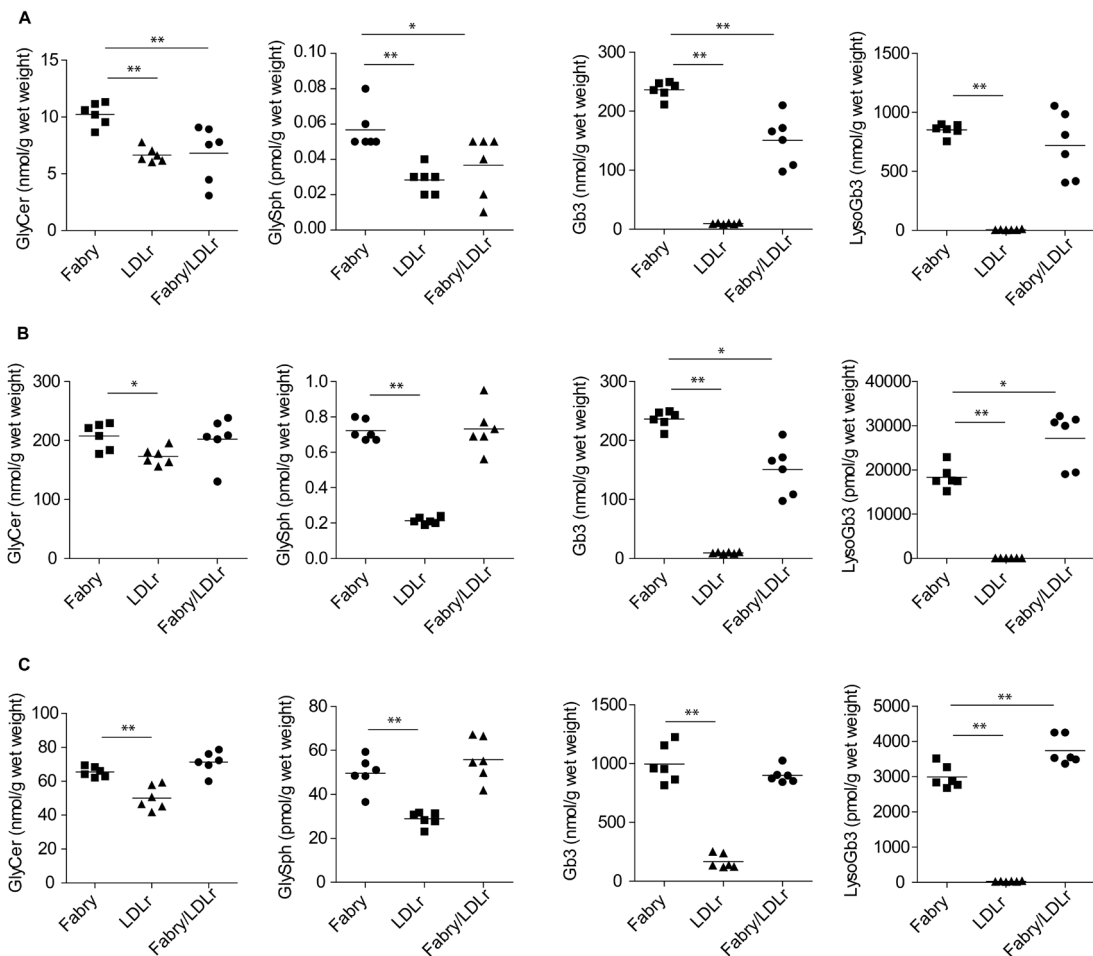
- [39] Y.-J. Shin, Y.J. Jeon, N. Jung, J.-W. Park, H.-Y. Park, S.-C. Jung, Substrate-specific gene expression profiles in different kidney cell types are associated with Fabry disease, *Mol. Med. Rep.* 12 (2015) 5049–5057.
- [40] S.K. Byeon, J.Y. Lee, J.-S. Lee, M.H. Moon, Lipidomic profiling of plasma and urine from patients with Gaucher disease during enzyme replacement therapy by nanoflow liquid chromatography–tandem mass spectrometry, *J. Chromatogr. A* 1381 (2015) 132–139.
- [41] D. Reczek, M. Schwake, J. Schröder, H. Hughes, J. Blanz, X. Jin, et al., LIMP-2 is a receptor for lysosomal mannose-6-phosphate-independent targeting of beta-glucocerebrosidase, *Cell* 131 (2007) 770–783.
- [42] A. Dardis, M. Filocamo, S. Grossi, G. Ciana, S. Franceschetti, S. Dominissini, et al., Biochemical and molecular findings in a patient with myoclonic epilepsy due to a mistarget of the beta-glucosidase enzyme, *Mol. Genet. Metab.* 97 (2009) 309–311.
- [43] V. Gieselmann, Lysosomal storage diseases, *Biochim. Biophys. Acta* 1270 (1995) 103–136.
- [44] T.M. Cox, M.B. Cachón-González, The cellular pathology of lysosomal diseases, *J. Pathol.* 226 (2012) 241–254.
- [45] E. Pavlova, S. Wang, J. Archer, N. Dekker, J. Aerts, S. Karlsson, et al., B cell lymphoma and myeloma in murine Gaucher's disease, *J. Pathol.* 231 (2013) 88–97.
- [46] H. Igisu, K. Suzuki, Progressive accumulation of toxic metabolite in a genetic leukodystrophy, *Science* 224 (1984) 753–755.
- [47] A.B. White, M.I. Givogri, A. Lopez-Rosas, H. Cao, R. van Breemen, G. Thinakaran, et al., Psychosine accumulates in membrane microdomains in the brain of krabbe patients, disrupting the raft architecture, *J. Neurosci.* 29 (2009) 6068–6077.
- [48] M. Zaka, D.A. Wenger, Psychosine-induced apoptosis in a mouse oligodendrocyte progenitor cell line is mediated by caspase activation, *Neurosci. Lett.* 358 (2004) 205–209.
- [49] K. Krabbe, A new familial, infantile form of diffuse brain-sclerosis, *Brain* 39 (1916) 74–114.
- [50] G.M. Pastores, Krabbe disease: an overview, *Int. J. Clin. Pharmacol. Ther.* 47 (Suppl. 1) (2009) S75–S81.
- [51] L.C. Castelvetti, M.I. Givogri, H. Zhu, B. Smith, A. Lopez-Rosas, X. Qiu, et al., Axonopathy is a compounding factor in the pathogenesis of Krabbe disease, *Acta Neuropathol.* 122 (2011) 35–48.
- [52] K. Subramanian, W.E. Balch, NPC1/NPC2 function as a tag team duo to mobilize cholesterol, *Proc. Natl. Acad. Sci. U. S. A.* 105 (2008) 15223–15224.
- [53] P.G. Pentchev, A.D. Boothe, H.S. Kruth, H. Weintraub, J. Stivers, R.O. Brady, A genetic storage disorder in BALB/C mice with a metabolic block in esterification of exogenous cholesterol, *J. Biol. Chem.* 259 (1984) 5784–5791.
- [54] E. Lloyd-Evans, F.M. Platt, Lipids on trial: the search for the offending metabolite in niemann-pick type C disease, *Traffic* 11 (2010) 419–428.
- [55] G.T. Besley, S.E. Moss, Studies on sphingomyelinase and beta-glucosidase activities in Niemann–Pick disease variants. Phosphodiesterase activities measured with natural and artificial substrates, *Biochim. Biophys. Acta* 752 (1983) 54–64.
- [56] M.T. Vanier, Biochemical studies in Niemann–Pick disease. I. Major sphingolipids of liver and spleen, *Biochim. Biophys. Acta* 750 (1983) 178–184.
- [57] R.W.D. Welford, M. Garzotti, C. Marques Lourenço, E. Mengel, T. Marquardt, J. Reunert, et al., Plasma lysosphingomyelin demonstrates great potential as a diagnostic biomarker for Niemann–Pick disease type C in a retrospective study, *PLoS One* 9 (2014), e114669.
- [58] P. Bauer, D.J. Balding, H.H. Klünemann, D.E.J. Linden, D.S. Ory, M. Pineda, et al., Genetic screening for Niemann–Pick disease type C in adults with neurological and psychiatric symptoms: findings from the ZOOM study, *Hum. Mol. Genet.* 22 (2013) 4349–4356.
- [59] A.-K. Giese, H. Mascher, U. Grittner, S. Eichler, G. Kramp, J. Lukas, et al., A novel, highly sensitive and specific biomarker for Niemann–Pick type C1 disease, *Orphanet J. Rare Dis.* 10 (2015) 78.
- [60] F.D. Porter, D.E. Scherrer, M.H. Lanier, S.J. Langmade, V. Molugu, S.E. Gale, et al., Cholesterol oxidation products are sensitive and specific blood-based biomarkers for Niemann–Pick C1 disease, *Sci. Transl. Med.* 2 (2010) 56ra81.



Supplemental Figure 1. Degradation of (lyso-)glycosphingolipids. Glycosphingolipids and respective lyso-glycosphingolipids (black) are degraded through the sequential action of lysosomal glycosidases (blue-bold). Deficiency in one of the glycosidases constitutes the molecular basis of lysosomal storage disorders (blue). GLA – α -galactosidase A, GLB1 – acid β -galactosidase, GBA – glucocerebrosidase, ASAHI – acid ceramidase, GALC – galactocerebrosidase.



Supplemental Figure 2. GBA activity is reduced in NPC mouse liver. GBA activity was measured with fluorogenic substrate in liver homogenates of end-stage *Npc1^{nih}* and *Npc1^{nmf164}* mice. Data representing mean \pm S.D. (n = 3-5) were analyzed by unpaired t-test. * $P < 0.05$, *** $P < 0.001$.



Supplemental Figure 3. LDLr deficiency in Fabry mice on a western-type diet does not exacerbate lipid abnormalities in spleen, heart and kidney.

Upper panel: Spleen (A), heart (B) and kidney (C) GSL (Gb3 and GlyCer) and lyso-GSL (lysoGb3 and GlySph) in male $Gla^{-/0}$ (Fabry), $Ldlr^{-/}$, and combined $Gla^{-/0}/Ldlr^{-/}$ – mice receiving western type diet. Data were analysed by Mann-Whitney u-test: * $P < 0.05$; ** $P < 0.01$.